TIPTEKNO'20 TIP TEKNOLOJİLERİ KONGRESİ
19-20 Kasım 2020
ONLINE

3D Femoral Head Detection in MRI Data Sequences with the Integro-differential Operator

Abbas Memiş[1], Songül Varlı[1], Fuat Bilgili[2]

[1]Department of Computer Engineering, Yıldız Technical University, İstanbul, Turkey
[2]Department of Orthopaedics and Traumatology, İstanbul University, İstanbul, Turkey
abbasmemis@gmail.com, svarli@yildiz.edu.tr, fuat.bilgili@istanbul.edu.tr

***Abstract*—This paper introduces a study of automatic femoral head detection in magnetic resonance imaging (MRI) data sequences. For the 3D detection of the multiform femoral heads having both spheric and aspheric shape structures, the three-dimensional form of the Integro-differential Operator (IDO) was performed. Following a set of image pre-processing operations including image intensity normalization, histogram equalization, morphological correction, hip joint separation and image binarization performed on bilateral hip MRI data sequences, the hip joints images are obtained in binary form in 3D. Then, the 3D form of IDO is performed in a predefined image volume to detect the femoral heads. Within the experimental studies performed on 8 bilateral hip MRI data sequences belonging to 6 Legg-Calve-Perthes disease (LCPD) patients, promising success rates were observed. In detection of a total of 16 femoral heads, 8 of which are spheric and 8 of which are aspheric, 0.7021 (±0.3160) and 0.6757 (±0.2989) DSC values measured for the spheric and aspheric femoral heads, respectively.**

***Keywords*—medical image processing; magnetic resonance imaging; 3D femoral head detection; integro-differential operator; Legg-Calve-Perthes disease.**

I. Introduction

Automatic detection and localization of the human body anatomical components in medical image modalities is one of the essential tasks in computerized medical image analysis. In the literature of medical image analysis, issue of anatomical object detection has been discussed and several reviews of research have been reported concerning the object detection in medical images [1], [2]. In the detection of the anatomical objects in medical images, non-learning-based methods and approaches could be performed as well as the learning-based approaches such as regression forests [3] and deep reinforcement learning [4].

In this paper, we focused on the 3D detection of the multiform femoral heads including both spheric and aspheric forms in magnetic resonance imaging (MRI) data sequences. In the current literature, various studies have been proposed for the challenge of femoral head and femur detection. Hough transforms [5] are commonly used for femoral head detection [6], [7] in 2D or 3D and they yield successful performance. In published research studies regarding the detection of femoral bone components, several methods such as knowledge-based algorithms [8], random forest regression voting [9], normalized score premised on the distribution of anatomical shape, size and presentation of the femur bone [10], shape detecting response function [11] were proposed. Additionally, femoral head detection was handled in our previous studies [12], [13], [14] by using Hough transforms. Moreover, we analyzed the performance of Integro-differential Operator (IDO) in femoral head detection in 2D [15] and promising detection results were achieved. In this study, we focused on the 3D detection of the femoral heads by performing IDO method on 3D MRI images. In this respect, the rest of the paper is organized as follows: Materials are given in Section II and methods are detailed in Section III. Experimental results observed in performance evaluations are presented in Section IV and conclusions of the proposed study are stated in Section V.

II. Materials

LCPD is a painful hip disorder which is seen in early childhood in pediatric orthopaedics. Its aetiology is still unclear and it causes significant bone loss and shape deformities in the global structure of the femoral head and proximal femur. As materials, 8 bilateral hip MRI data sequences belonging to 6 male Legg-Calve-Perthes disease (LCPD) patients were used within the scope of this study. The mean age of the patients in the study cohort is 8 (±4) years, and the mean body mass is 34 (±15.23) kg. All the MRI data sequences were acquired by a 1.5T MRI scanner (Achieva & Intera, Philips Medical Systems) in coronal imaging plane. Ground truth values of the 3D center coordinates and sphere radius of the femoral heads are determined manually under the guidance of an expert clinician via ITK-SNAP medical image segmentation software tool [16]. As a result of manually marking process, ground truth 3D center coordinates and radii of the femoral head spheres were obtained. In all bilateral coronal MRI data sequences, one of the femoral heads is healthy and the other one is pathological. Hence, we have a total of 16 single hip joints, 8 of which are spheric (healthy) and 8 of which are aspheric (pathological). The mean radius of the healthy and pathological femoral heads are 19.67 (±2.24), 19.65 (±2.85) respectively. The pathological femoral heads of the patients have different severity of the disease and therefore, the shape deformity rates are different from each

978-1-7281-8073-1/20/ $31.00 © 2020 IEEE

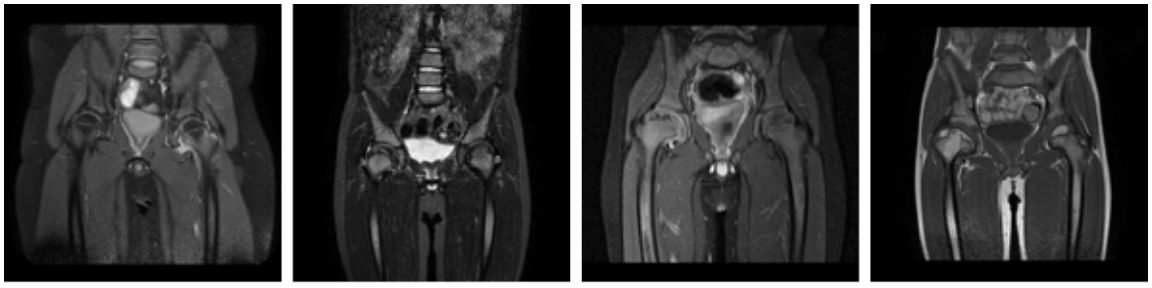

Fig. 1: Sample MRI slices from the evaluated LCPD MRI dataset (Disease levels are Initial (left hip joint), Fragmentation (right hip joint), Reossification (right hip joint) and Remodelling (right hip joint) respectively).

TABLE I: Clinical statistics of the patient cohort.

Patient ID	Age (year)	Body mass (kg.)	Disease stage	MRI Seq. (#)
Patient-1	3	14	Reossification	1
Patient-2	4	20	Fragmentation	1
Patient-3	9	30	Remodelling	1
Patient-4	9	40	Remodelling	1
Patient-5	13	50	Initial	2
Patient-6	9	50	Remodelling	2
μ ($\pm\sigma$)	8 ($\pm$4)	34 ($\pm$15.23)		

other. According to the Waldenstrom radiological classification system, the disease consists of 4 stages as Level-1 (Initial), Level-2 (Fragmentation), Level-3 (Reossification) and Level-4 (Remodelling). All the clinical statistics of the patient cohort are presented in Table I. Additionally, sample MRI slices from the evaluated MRI dataset are shown in Figure 1.

III. Methods

A. MRI Data Pre-processing

In the implementation of the IDO based 3D femoral head detection, it was determined to perform the IDO method on binary images instead of the MRI intensity images due to the high tissue complexity which may make it harder to detect the target object in the MRI data sequences. For this purpose, a set of image pre-processing operations consisting of 5 stages as image intensity normalization (normalization range [0,1]), histogram equalization (equalization range [0,255]), morphological correction (regional image filling based on Matlab "imfill" function), hip joint separation (vertically separation of MRI slices into two halves) and image binarization (binary thresholding) was performed on the consecutive slices of the bilateral hip MRI data sequences. Finally, the hip joints images are obtained in binary form in 3D. In Figure 2, resultant femoral head RoIs (region of interests) which were observed after each MRI data pre-processing stage are presented.

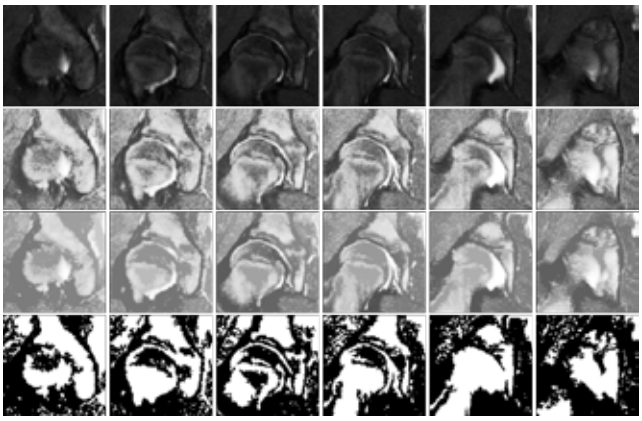

Fig. 2: Image pre-processing operations on consecutive MRI slices and the resultant RoIs (region of interests) of the femoral head heads (1st **row:** image intensity normalization, 2nd **row:** histogram equalization, 3rd **row:** morphological correction, 4th **row:** image binarization after hip joint separation).

B. 3D Femoral Head Detection with the Three-dimensional Integro-differential Operator (IDO)

IDO [17] was firstly introduced by J.Daugman to localize the iris and pupil in recognition of the iris biometric. In its original form, it is performed to find the center coordinates and radii of the circular structures in 2D by maximizing the difference of the sum of the intensities of consecutive circles within a radius range of $[R_{min},R_{max}]$. In this study, the related operator was rearranged in 3D to handle the detection of femoral head spheres. In 3D, consecutive spheres are drawn instead of the circles for the detection of the spherical structures as similar to 2D. In Equation (1), 3D form of the IDO is given as follows:

$$max(r, x_0, y_0, z_0) \left| G_\sigma(r) * \frac{\partial}{\partial r} \oint_{r,x_0,y_0,z_0} \frac{I(x,y,z)}{4\pi r^2} ds \right| \quad (1)$$

where $I(x,y,z)$ is a 3D binary input image data, (x_0, y_0, z_0) is the assumed center coordinate of the femoral head sphere,

r is the radius of the circles with the center coordinate at (x_0, y_0, z_0), s denotes the contour of the sphere given by the parameters (r, x_0, y_0, z_0), and $G_\sigma(r)$ is a Gaussian smoothing function with the standard deviation σ. By taking any pixel on an image as a center point, spheres are drawn for each radius value within a certain radius range. Then, the sum of the intensity values on each sphere is calculated and these sum values are stored in a vector. The consecutive differences of the elements in this sum vector are calculated and the difference vector is smoothed by using a 1D Gaussian filter with a predefined standard deviation. The maximum value in the difference vector gives the position where the colour difference is largest i.e., the radius of the sphere to be detected. These operations described above are performed on each pixel in an image, and the most probable sphere is determined by finding the position and radius value at which the greatest difference value of the intensity sums over consecutive spheres is obtained. In detection of the femoral head spheres, 3D IDO is performed by defining consecutive sphere surfaces via conventional sphere notations in Equation (2) within a predefined radius range of $[R_{min}, R_{max}]$ as delineated in Figure 3. In Equation (2), (C_x, C_y, C_z) is a center point and r is the radius of the sphere. (P_x, P_y, P_z) is a sphere surface point with the azimuth angle of θ and elevation angle of φ.

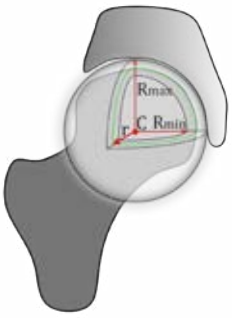

Fig. 3: A femoral head sphere with a center of C and a radius of r, and illustration of a radius range of $[R_{min}, R_{max}]$ on it.

$$\begin{aligned} P_x &= C_x + (r \cdot \cos(\varphi) \cdot \cos(\theta)) \\ P_y &= C_y + (r \cdot \cos(\varphi) \cdot \sin(\theta)) \\ P_z &= C_z + (r \cdot \sin(\varphi)) \end{aligned} \tag{2}$$

C. Evaluation Metrics

In performance evaluation of the proposed study, two evaluation metrics were used. The first one is the Root Mean Square Error (RMSE), and the second one is the Dice Similarity Coefficient (DSC). The RMSE metric was utilized to measure the error of the radius and center coordinate of the detected femoral head spheres. In Equation (3), the notation of the RMSE is given as follows:

$$RMSE = \sqrt{\frac{1}{N}\sum_{i=1}^{N}(A_i - P_i)^2} \tag{3}$$

where A and P denote the ground truth and predicted sphere parameters respectively. N is the dimension of the vectors A and P and has a value of 2 in the error measurement of the center coordinate and 1 in the error measurement of the radius. By using the center coordinates and radii, it is possible to define spherical structures in image spatial domain. Hence, the degree of the similarity of the actual and predicted femoral head spheres can be calculated by using the DSC:

$$DSC(S_A, S_P) = \frac{2|S_A \cap S_P|}{|S_A| + |S_P|} \tag{4}$$

where S_A is the actual femoral head sphere, and S_P is the predicted femoral head sphere. The volume criterion is based on the number of the voxels within the sphere. Therefore, the $DSC(S_A, S_P)$ value indicates the degree of the overlap of two domains. If it is close to 1, it indicates that the actual and predicted femoral head spheres are quite similar. On the other hand, the similarity of the actual and predicted femoral head spheres is low if the DSC value is close to 0.

IV. Results

Performance evaluation of the proposed study was carried out on 8 bilateral hip MRI data sequences belonging to 6 LCPD patients and a total of 16 femoral heads, 8 of which are spheric and 8 of which are aspheric, were evaluated in detection of the femoral head spheres in 3D by using IDO. In the implementation of the IDO, a three-dimensional range cube is defined on the 3D MRI data and only the IDO maximum difference values of the consecutive spheres were taken into consideration within this predefined cube with the size of $[w/3, 2w/3]$, $[h/3, 2h/3]$, $[d-2, d+2]$, where variables of w, h, d are the image block width, image block height and the number of the MR image sections, to decrease the processing time and eliminate the false positive spheres that could be possibly detected as femoral head within the area outside the specified cube. In Figure 4, the IDO maximum difference values of the consecutive spheres are illustrated as density maps in which the red and black colours (close to 0) indicate the non-spherical objects, and the white and yellow colours (close to 1) indicate the centers of the spherical objects.

In Table II, the RMSE and DSC values observed in 3D detection of the spheric and aspheric femoral heads are presented. As seen in Table II, quite successful detection rates were achieved except the sample 5 and 6. The extremely poor performance seen in the relevant MRI sequences also decreased the mean success rates and increased their standard deviations. Additionally, the observed results were compared with the outcomes of our previous work [14] in which the same MRI data sequences were evaluated in detection of the femoral head spheres by using Spherical Hough Transform (SHT). As seen in Table III, more successful results were obtained with SHT compared to the IDO method in 3D.

V. Conclusion

In this paper, a study of automatic femoral head detection in MRI data sequences was introduced. By performing the IDO

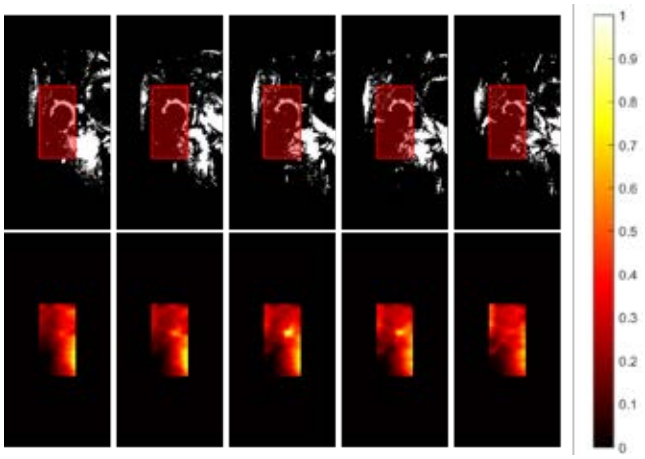

Fig. 4: Density maps of the IDO maximum difference values of the consecutive spheres (**red** and **black** colours (close to 0) indicate the non-spherical objects, and the **white** and **yellow** colours (close to 1) indicate the potential spheres).

TABLE II: The observed RMSE and DSC values for the spheric and aspheric femoral heads in 3D femoral head detection with IDO.

	Spheric Femoral Heads			Aspheric Femoral Heads		
MRI Sequence No	RMSE center (mm.)	RMSE radius (mm.)	DSC	RMSE center (mm.)	RMSE radius (mm.)	DSC
1	5.50	0.09	0.7492	2.15	0.83	0.8821
2	0.00	0.59	0.9467	1.68	0.77	0.9050
3	4.70	1.06	0.8348	8.12	0.16	0.7320
4	7.47	0.74	0.7401	6.85	0.74	0.7604
5	17.26	0.47	0.4647	40.07	0.12	0.0124
6	39.26	1.09	0.0246	16.96	1.90	0.4865
7	1.06	0.86	0.9381	7.04	0.13	0.7583
8	2.36	0.04	0.9186	3.81	0.01	0.8692
mean	9.70	0.62	0.7021	10.83	0.58	0.6757
±std.	13.10	0.40	0.3160	12.75	0.63	0.2989

TABLE III: Performance comparison of the Spherical Hough Transform (SHT) and Integro-differential Operator (IDO) in 3D detection of the spheric and aspheric femoral heads.

	Spheric Femoral Head			Aspheric Femoral Head		
Method	RMSE center (mm.)	RMSE radius (mm.)	DSC	RMSE center (mm.)	RMSE radius (mm.)	DSC
SHT | mean	2.14	0.84	0.8992	5.53	0.71	0.8006
(±std.)	1.74	0.56	0.0608	4.29	0.36	0.1355
IDO | mean	9.70	0.62	0.7021	10.83	0.58	0.6757
(±std.)	13.10	0.40	0.3160	12.75	0.63	0.2989

approach in 3D, promising detection rates were achieved. In 3D detection of the spheric and aspheric femoral heads in 8 MRI data sequences of 6 LCPD patients affected unilaterally, 9.70 mm. (± 13.10 mm.) mean RMSE for center coordinates, 0.62 mm. (± 0.40 mm) mean RMSE for radii, 0.7021 (± 0.3160) mean DSC were observed on spheric femoral heads and 10.83 mm. (± 12.75 mm.) mean RMSE for center coordinates, 0.58 mm. (± 0.63 mm.) mean RMSE for radii, 0.6757 (± 0.2989) mean DSC were observed on aspheric femoral heads.

REFERENCES

[1] S. K. Zhou, "A survey of anatomy detection," in *Medical Image Recognition, Segmentation and Parsing*. Elsevier, 2016, pp. 25–44.
[2] S. K. Zhou, "Discriminative anatomy detection: Classification vs regression," *Pattern Recognition Letters*, vol. 43, pp. 25–38, 2014.
[3] A. Criminisi, D. Robertson, E. Konukoglu, J. Shotton, S. Pathak, S. White, and K. Siddiqui, "Regression forests for efficient anatomy detection and localization in computed tomography scans," *Medical image analysis*, vol. 17, no. 8, pp. 1293–1303, 2013.
[4] F. Navarro, A. Sekuboyina, D. Waldmannstetter, J. C. Peeken, S. E. Combs, and B. H. Menze, "Deep reinforcement learning for organ localization in CT," *arXiv preprint arXiv:2005.04974*, 2020.
[5] P. Mukhopadhyay and B. B. Chaudhuri, "A survey of Hough transform," *Pattern Recognition*, vol. 48, no. 3, pp. 993–1010, 2015.
[6] Y. Chen, X. Ee, W. K. Leow, and T. S. Howe, "Automatic extraction of femur contours from hip x-ray images," in *International Workshop on Computer Vision for Biomedical Image Applications*. Springer, 2005, pp. 200–209.
[7] H. Ruppertshofen, D. Künne, C. Lorenz, S. Schmidt, P. Beyerlein, Z. Salah, G. Rose, and H. Schramm, "Multi-level approach for the discriminative generalized Hough transform," in *CURAC 2011: 10. Jahrestagung der Deutschen Gesellschaft für Computer-und Roboterassistierte Chirurgie, Magdeburg, Germany, 15-16 September 2011*. CURAC, 2011.
[8] R. Pilgram, C. Walch, M. Blauth, W. Jaschke, R. Schubert, and V. Kuhn, "Knowledge-based femur detection in conventional radiographs of the pelvis," *Computers in Biology and Medicine*, vol. 38, no. 5, pp. 535–544, 2008.
[9] C. Lindner, S. Thiagarajah, J. M. Wilkinson, G. A. Wallis, T. F. Cootes, arcOGEN Consortium *et al.*, "Accurate fully automatic femur segmentation in pelvic radiographs using regression voting," in *International Conference on Medical Image Computing and Computer-Assisted Intervention*. Springer, 2012, pp. 353–360.
[10] P. Mukherjee, G. Swamy, M. Gupta, U. Patil, and K. B. Krishnan, "Automatic detection and measurement of femur length from fetal ultrasonography," in *Medical Imaging 2010: Ultrasonic Imaging, Tomography, and Therapy*, vol. 7629. International Society for Optics and Photonics, 2010, p. 762909.
[11] S.-J. Liu, Z. Zou, S.-D. Luo, and S.-H. Liao, "A novel harmonic field based method for femoral head segmentation from challenging CT data," in *2016 Third International Conference on Computing Measurement Control and Sensor Network (CMCSN)*. IEEE, 2016, pp. 92–95.
[12] A. Memiş, S. Albayrak, and F. Bilgili, "Femoral head detection in Perthes MR slices with circular Hough transform," in *2018 26th Signal Processing and Communications Applications Conference (SIU)*. IEEE, 2018, pp. 1–4.
[13] A. Memiş, S. Albayrak, and F. Bilgili, "A new scheme for automatic 2D detection of spheric and aspheric femoral heads: A case study on coronal MR images of bilateral hip joints of patients with Legg-Calve-Perthes disease," *Computer methods and programs in biomedicine*, vol. 175, pp. 83–93, 2019.
[14] A. Memiş, S. Albayrak, and F. Bilgili, "3D detection of spheric and aspheric femoral heads in coronal MR images of patients with Legg-Calve-Perthes disease using the spherical Hough transform," in *Proceedings of the 2018 3rd International Conference on Biomedical Imaging, Signal Processing*, 2018, pp. 46–52.
[15] A. Memiş, S. Varlı, and F. Bilgili, "Computerized 2D detection of the multiform femoral heads in magnetic resonance imaging (MRI) sections with the integro-differential operator," *Biomedical Signal Processing and Control*, vol. 54, p. 101578, 2019.
[16] P. A. Yushkevich, J. Piven, H. C. Hazlett, R. G. Smith, S. Ho, J. C. Gee, and G. Gerig, "User-guided 3D active contour segmentation of anatomical structures: significantly improved efficiency and reliability," *Neuroimage*, vol. 31, no. 3, pp. 1116–1128, 2006.
[17] J. Daugman, "How iris recognition works," in *The essential guide to image processing*. Elsevier, 2009, pp. 715–739.